

First Amplitude Analysis of $D^0 \rightarrow K^- \pi^0 e^+ \nu_e$ and Observation of $D^0 \rightarrow K_2^*(1430)^- e^+ \nu_e$

M. Ablikim *et al.**

(BESIII Collaboration)

(Dated: February 28, 2026)

We present the first amplitude analysis of the semileptonic decay $D^0 \rightarrow K^- \pi^0 e^+ \nu_e$ by analyzing $e^+ e^-$ annihilation data corresponding to an integrated luminosity of 20.3 fb^{-1} collected at the center-of-mass energy of 3.773 GeV with the BESIII detector. A tiny \mathcal{D} -wave component of the $K_2^*(1430)^-$ accounting for $(0.16 \pm 0.05_{\text{stat}} \pm 0.02_{\text{syst}})\%$ of the $K^- \pi^0$ is observed for the first time with a significance of 7.9σ in addition to the dominant \mathcal{P} -wave component of $K^*(892)^-$ and the sub-dominant $K^- \pi^0$ \mathcal{S} -wave. The hadronic form factors of the $D^0 \rightarrow K^*(892)^-$ transition are measured precisely as $r_V = V(0)/A_1(0) = 1.41 \pm 0.05_{\text{stat}} \pm 0.01_{\text{syst}}$ and $r_2 = A_2(0)/A_1(0) = 0.77 \pm 0.04_{\text{stat}} \pm 0.02_{\text{syst}}$. The branching fraction of $D^0 \rightarrow K^*(892)^- e^+ \nu_e$ with $K^*(892)^- \rightarrow K^- \pi^0$ is measured to be $(7.403 \pm 0.061_{\text{stat.}} \pm 0.048_{\text{syst.}}) \times 10^{-3}$. Combining the measurements of the $D^0 \rightarrow K^*(892)^- (K^*(892)^- \rightarrow K^- \pi^0) \ell^+ \nu_\ell$, lepton flavor universality is tested by the ratio $\mathcal{R}_{\text{LFU}} = \mathcal{B}(D^0 \rightarrow K^*(892)^- \mu^+ \nu_\mu) / \mathcal{B}(D^0 \rightarrow K^*(892)^- e^+ \nu_e) = 0.928 \pm 0.020_{\text{stat}} \pm 0.012_{\text{syst}}$ with unprecedented precision; no violation is found. Furthermore, isospin symmetry in the decay $K^*(892)^- \rightarrow K\pi$ is tested by $\mathcal{R}_{K^*-} = \mathcal{B}(K^*(892)^- \rightarrow K^- \pi^0) / \mathcal{B}(K^*(892)^- \rightarrow K_S^0 \pi^-) = 1.09 \pm 0.02_{\text{stat}} \pm 0.02_{\text{syst}}$ for the first time using the previous measurement of $D^0 \rightarrow K^*(892)^- e^+ \nu_e$ with $K^*(892)^- \rightarrow K_S^0 \pi^-$. Finally, the phase shift of the $K\pi$ \mathcal{S} -wave is extracted in a model-independent way, which sheds light on the nature of the lightest strange scalar meson, the $K_0^*(700)$.

Semileptonic (SL) decays of charmed mesons provide a good platform to study the non-perturbative regime of quantum chromodynamics (QCD), test lepton flavor universality (LFU), and extract Cabibbo-Kobayashi-Maskawa (CKM) matrix elements [1, 2]. In particular, the four-body SL decay $D \rightarrow K\pi\ell\nu_\ell$ (denoted as $D_{\ell 4}$) has been the subject of much theoretical work [3–16] and experimental measurements [17–26]. These decays offer an excellent opportunity to directly test theoretical methods with precise measurements, thereby deepening our understanding of the Standard Model (SM). They also contain abundant dynamical information on the $K\pi$ system, making them well-suited for studying strange mesons such as the $K_0^*(700)$ (also known as κ), $K^*(892)$, and $K_2^*(1430)$ [27], and so on. However, the decay $D^0 \rightarrow K^- \pi^0 e^+ \nu_e$ was only searched by MARK-III without observation in 1991 [17]. Now, it is time to study this decay with a large dataset at BESIII [28, 29].

The tensor mesons, $K_2^*(1430)$ and $a_2(1320)$, as well as the two isosinglet mesons, $f_2(1270)$ and $f_2'(1525)$, collectively form the 1^3P_2 nonet [27] in the quark model. Recently, using SU(3) flavor symmetry, the branching fractions (BFs) of $D^0 \rightarrow K_2^*(1430)^- \ell^+ \nu_\ell$ have been predicted to be $(1.36 \pm 0.49) \times 10^{-5}$ and $(0.91 \pm 0.31) \times 10^{-5}$ for positron and muon channels, respectively [30]. In comparison, the corresponding predictions from the relativistic quark model (RQM) are $(1.26 \pm 0.14) \times 10^{-5}$ and $(0.81 \pm 0.09) \times 10^{-5}$ [31]. Although numerous analyses have been conducted on the $D_{\ell 4}$ decays, there was still no observation for $K_2^*(1430)$ in the previous studies [20–26]. Any observation of $K_2^*(1430)$ in the $D_{\ell 4}$ decays is crucial to test these predictions.

The \mathcal{P} -wave component of $K^*(892)$ dominates the $K\pi$ system in the $D_{\ell 4}$ decays [18–26]. Many theoretical calculations on $D^0 \rightarrow K^*(892)^- \ell^+ \nu_\ell$ have been performed by various QCD models including Lattice QCD (LQCD) [5], light-cone sum rules (LCSR) [7, 13, 16], constituent quark model

(CQM) [11], heavy quark effective theory (HQET) [4], combined heavy meson and chiral theory (HM χ T) [6], covariant light-front quark model (CLFQM) [8, 10], large energy chiral quark model (LE χ QM) [9], covariant confined quark model (CCQM) [12] and RQM [14]. However, there are still significant discrepancies on the form factor (FF) predictions among these models. Therefore, precision measurements of these FFs are desirable.

Previously, there were 2-3 σ tensions [32–36] reported in various LFU tests in SL B decays by the LHCb, Belle and BABAR experiments. Precision measurements of the ratio $\mathcal{R}_{\text{LFU}} = \frac{\mathcal{B}(D^0 \rightarrow K^*(892)^- \mu^+ \nu_\mu)}{\mathcal{B}(D^0 \rightarrow K^*(892)^- e^+ \nu_e)}$ in the $D_{\ell 4}$ decays provide critical and complementary tests of LFU in the weak interaction and could reveal new physics effects. Additionally, it may be surprising that there is no measurement of the BFs of $K^*(892)^- \rightarrow K^- \pi^0$ and $K^*(892)^- \rightarrow K_S^0 \pi^-$ since the $K^*(892)$ discovery in 1961 [37]. The value is usually taken as $\simeq 1/3$, ignoring isospin-breaking effects. Theoretically, these effects are naively expected to be at most a few percent, but this has never been tested experimentally. The SL decay $D^0 \rightarrow K^*(892)^- \ell^+ \nu_\ell$ provides a unique arena to perform the test via the ratio $\mathcal{R}_{K^*-} = \frac{\mathcal{B}(K^*(892)^- \rightarrow K^- \pi^0)}{\mathcal{B}(K^*(892)^- \rightarrow K_S^0 \pi^-)}$ = $\frac{\mathcal{B}(D^0 \rightarrow K^*(892)^- \ell^+ \nu_\ell) \mathcal{B}(K^*(892)^- \rightarrow K^- \pi^0)}{\mathcal{B}(D^0 \rightarrow K^*(892)^- \ell^+ \nu_\ell) \mathcal{B}(K^*(892)^- \rightarrow K_S^0 \pi^-)}$.

Finally, the $K^- \pi^0$ system contains a significant \mathcal{S} -wave component, whose properties can shed light on the nature of scalar mesons, particularly the long-standing puzzle of the $K_0^*(700)$ [38]. This resonance is a member of the lightest scalar meson nonet, together with the $f_0(500)$ (also known as σ), $f_0(980)$, and $a_0(980)$ [38–41]. The pole parameters of the $K_0^*(700)$ have been extracted through dispersion relations [42–44], based on the only two datasets of the phase shift [45, 46]. Thus, an additional measurement of the $K\pi$ phase shift in a clean environment is also valuable to constrain the pole parameters of the $K_0^*(700)$.

*Full author list given at the end of the Letter.

This Letter reports the first dynamics study and BF measurement of $D^0 \rightarrow K^- \pi^0 e^+ \nu_e$ using 20.3 fb^{-1} of $e^+ e^-$ collision data collected at the center-of-mass energy of $\sqrt{s} = 3.773 \text{ GeV}$ with the BESIII detector. An amplitude analysis is used to decompose the $K^- \pi^0$ system into the $K_0^*(700)^-$ and $K_0^*(1430)^-$ S -wave components, the $K^*(892)^-$ P -wave component, the $K^*(1410)^-$ P' -wave component, and the $K_2^*(1430)^-$ D -wave component. Charge-conjugate modes are implied throughout this Letter.

A detailed description of the design and performance of the BESIII detector is available in Refs. [47, 48]. An inclusive Monte Carlo (MC) sample, as outlined in Refs. [21], is utilized to determine selection efficiencies and estimate background contributions. This inclusive MC sample includes the production of $D\bar{D}$, non- $D\bar{D}$ decays of the $\psi(3770)$, the initial state radiation production of the J/ψ and $\psi(3686)$, and continuum processes. In the generation of the signal, $D^0 \rightarrow K^- \pi^0 e^+ \nu_e$, we take into account the knowledge of the amplitude results obtained in this work.

Near open-charm threshold at $\sqrt{s} = 3.773 \text{ GeV}$, $D\bar{D}$ mesons are produced in pairs. The \bar{D}^0 (single-tag, ST) is fully reconstructed first in three channels $\bar{D}^0 \rightarrow K^+ \pi^-$, $\bar{D}^0 \rightarrow K^+ \pi^- \pi^0$, and $\bar{D}^0 \rightarrow K^+ \pi^- \pi^- \pi^+$. In the presence of the ST \bar{D}^0 , the $D^0 \rightarrow K^- \pi^0 e^+ \nu_e$ decay is reconstructed from the remaining tracks recoiling against the \bar{D}^0 meson to form double-tag (DT) candidates. More details of this DT method are given in Appendix A. Detailed descriptions of the selection criteria for π^\pm , K^\pm , e^\pm , γ , and π^0 candidates are provided in Ref. [21].

To separate ST \bar{D}^0 mesons from combinatorial backgrounds, a beam-constrained mass defined as $M_{\text{BC}} = \sqrt{(\sqrt{s}/2)^2/c^4 - |\vec{p}_{\bar{D}^0}|^2/c^2}$ is used, where $\vec{p}_{\bar{D}^0}$ represents the momentum of the \bar{D}^0 meson candidate. To improve signal significance, the kinematic variable $|\Delta E| = |E_{\bar{D}^0} - \sqrt{s}/2|$ is required to be within a certain range for each mode. Here $E_{\bar{D}^0}$ is the energy of the \bar{D}^0 candidate. For each ST mode and charm, if multiple \bar{D}^0 candidates are found in an event, only the one with the minimum $|\Delta E|$ is retained for further analysis. The \bar{D}^0 meson yields in each mode are determined through a binned maximum likelihood fit to the M_{BC} distributions. The signal is modeled using the MC simulated shape convolved with a double Gaussian function, while an ARGUS function describes the combinatorial background. The total \bar{D}^0 yield is $N_{\text{ST}}^{\text{tot}} = (15375 \pm 4) \times 10^3$. Details of $|\Delta E|$ and M_{BC} requirements, efficiencies, and yields in each ST mode are listed in Supplemental Material [49].

The missing neutrino, ν_e , in the D^0 reconstruction can be characterized by the variable $U_{\text{miss}} = E_{\text{miss}} - |\vec{p}_{\text{miss}}|c$, where E_{miss} and \vec{p}_{miss} are the energy and momentum of the missing neutrino inferred from energy and momentum conservation [21], respectively. To suppress backgrounds, several selection criteria are imposed. The backgrounds of $D^0 \rightarrow K^- e^+ \nu_e$ and $D^0 \rightarrow K^- \pi^+ \pi^0$ are rejected by two requirements of $U_{\text{miss}}^\pi > 0.04 \text{ GeV}$ and $M_{K^- \pi^0 e^+} < 1.70 \text{ GeV}/c^2$. Here, U_{miss}^π is analogous to U_{miss} but with the π^0 candi-

date excluded from the final state (i.e., it peaks at zero for $D^0 \rightarrow K^- e^+ \nu_e$ decays) and $M_{K^- \pi^0 e^+}$ represents the invariant mass of the $K^- \pi^0 e^+$ system. A further background arises due to the exchange of the π^0 from $D^- \rightarrow K^+ \pi^- \pi^- \pi^0$ with the π^+ from $D^+ \rightarrow K^- \pi^+ e^+ \nu_e$. A quantity $M_{\text{BC}}^{\text{new}}$, defined for the decay $D^- \rightarrow K^+ \pi^- \pi^- \pi^0$, is required to lie outside $(1.863, 1.877) \text{ GeV}/c^2$. After applying all selection criteria, the signal yield is extracted through an unbinned maximum likelihood fit to the U_{miss} distribution. In the fit, the signal is modeled using the signal MC simulated shape, while the background is derived from the inclusive MC sample, and both are convolved with a Gaussian smearing function. All parameters are free in the fit, shown in Fig. 1, and the signal yield is determined to be 28900 ± 224 .

The averaged D^0 reconstruction efficiency is $(24.90 \pm 0.02)\%$, including a correction due to the combined discrepancy between data and MC simulation. The BF of $D^0 \rightarrow K^- \pi^0 e^+ \nu_e$ is determined to be $(7.878 \pm 0.063_{\text{stat.}} \pm 0.048_{\text{syst.}}) \times 10^{-3}$ based on the DT method described in Appendix A, where the first uncertainty is statistical and the second is systematic. The dominant systematic uncertainties on the BF arise from the U_{miss} fit and efficiency differences between data and MC simulation. By varying the combinatorial background shape, an uncertainty from the U_{miss} fit of 0.3% is determined. The uncertainties due to tracking and PID for the e^+ , 0.14%, and the K^- , 0.14%, as well as π^0 reconstruction, 0.2%, are evaluated using $e^+ e^- \rightarrow \gamma e^+ e^-$ events and DT $D\bar{D}$ hadronic events [24], respectively. The uncertainty from ST reconstruction, 0.3%, is from Ref. [24]. The uncertainties associated with the $M_{K^- \pi^0 e^+}$ (0.1%), U_{miss}^π (0.1%), and $M_{\text{BC}}^{\text{new}}$ (0.2%) requirements are estimated by smearing the signal MC sample. In the BF calculation, the BF of $\pi^0 \rightarrow \gamma\gamma$ is taken as $(98.823 \pm 0.034)\%$ [27], with its uncertainty propagated accordingly. Furthermore, the uncertainty in MC statistics is determined to be 0.1%. The total systematic uncertainty of BF is 0.6%, from the sum of all contributions in quadrature.

To study the dynamics of $D^0 \rightarrow K^- \pi^0 e^+ \nu_e$, the candidate events are further required to be within $U_{\text{miss}} \in (-0.06, 0.06) \text{ GeV}$, while the maximum energy of additional photons $E_{\text{extra}\gamma}^{\text{max}}$ unrelated to the π^0 in both tag and signal sides is required to be less than 0.4 GeV. A sample of 25665 candidate events with a purity of $(94.5 \pm 0.14)\%$ is obtained.

The differential decay width for $D_{\ell 4}$ decays is given in Ref. [20, 50], and can be expressed in terms of five kinematic variables $m_{K^- \pi^0}$, q , $\cos \theta_K$, $\cos \theta_e$ and χ [50]. The variables $m_{K^- \pi^0}$ and q are the invariant masses of $K^- \pi^0$ and $e^+ \nu_e$, respectively. There are two helicity angles, the decay angle θ_K between the K^- flight direction in the $K^- \pi^0$ rest frame and the $K^- \pi^0$ system boost direction in the D^0 frame, and θ_e , defined analogously for the $e^+ \nu_e$ system. The acoplanarity angle χ is the orientation between the decay planes of the $K^- \pi^0$ and $e^+ \nu_e$. The S , P , P' and D -wave contributions are considered in the amplitude analysis. The S -wave phase employs the LASS parameterization [45] $\delta_S(m_{K^- \pi^0}) = \delta_{\text{BG}} + \delta_{K_0^*(1430)^-}$, incorporating the contributions from $K_0^*(1430)^-$

and other components. δ_{BG} is a function of scattering length $a_{\mathcal{S},\text{BG}}^{1/2}$ and effective range $b_{\mathcal{S},\text{BG}}^{1/2}$. The magnitude of the \mathcal{S} -wave, $\mathcal{A}_{\mathcal{S}}$, is a function of the dimensionless coefficient $r_{\mathcal{S}}^{(1)}$ and the relative intensity $r_{\mathcal{S}}$ [20]. The \mathcal{P} , \mathcal{P}' and \mathcal{D} -wave amplitudes are described by the Breit-Wigner functions with a parameter r_{BW} , which is the effective radius of the strong-interaction barrier, and the masses and widths of the $K\pi$ resonances [20]. Moreover, the helicity FFs can in turn be related to the two axial-vector FFs $A_1(q^2)$, $A_2(q^2)$, and a vector FF $V(q^2)$ for the \mathcal{P} , \mathcal{P}' waves. The FFs of the \mathcal{D} -wave also include two axial-vector and one vector FFs, $T_1(q^2)$, $T_2(q^2)$ and $T_V(q^2)$. All of them are parametrized with the simple pole form, with pole masses m_A and m_V . At $q^2 = 0$, the FF ratios $r_V = V(0)/A_1(0)$ and $r_2 = A_2(0)/A_1(0)$ are determined from the fit. For the $K_2^*(1430)^-$, only the amplitude magnitude $r_{\mathcal{D}}$ and phase $\phi_{\mathcal{D}}$ are floated, while the FFs $r_{2V} = T_V(0)/T_1(0)$ and $r_{22} = T_2(0)/T_1(0)$ are fixed to 1 [51, 52], and the masses and widths of $K^*(1410)^-$ and $K_2^*(1430)^-$ are fixed to their PDG values [27].

The amplitude analysis is performed on the differential decay width using the unbinned maximum likelihood fit method. The negative log-likelihood function is defined as

$$-\ln \mathcal{L} = - \sum_{i=1}^N \left[(1 - f_b) \frac{\omega(\xi, \eta)}{\int d\xi \omega(\xi, \eta) \epsilon(\xi) R_4(\xi_i)} + f_b \frac{B_\epsilon(\xi)}{\int d\xi B_\epsilon(\xi) \epsilon(\xi) R_4(\xi_i)} \right], \quad (1)$$

where f_b is the background fraction obtained from the U_{miss} fit, $\omega(\xi, \eta)$ represents the signal probability density function (PDF) described by the intensity distribution [21], and $B_\epsilon(\xi)$ denotes the efficiency-corrected background PDF described by the inclusive MC sample. The efficiency $\epsilon(\xi)$ is evaluated using the signal MC sample generated in phase space, by binning the five-dimensional variables and calculating the efficiency in each bin, and $R_4(\xi_i)$ is an element of four-body phase space. Here, ξ and η correspond to the five-dimensional kinematic variables and the fit parameters, respectively. The integrals in the denominators are performed using the same signal MC samples used for signal and background PDFs.

The statistical significances of the \mathcal{D} and \mathcal{P}' waves are evaluated via the likelihood ratio $\Lambda_{\mathcal{D}} = -2 \ln(\mathcal{L}_{\mathcal{SP}}/\mathcal{L}_{\mathcal{SPD}})$ and $\Lambda_{\mathcal{P}'} = -2 \ln(\mathcal{L}_{\mathcal{SPD}}/\mathcal{L}_{\mathcal{SPDP}'})$, respectively, where $\mathcal{L}_{\mathcal{SP}}$, $\mathcal{L}_{\mathcal{SPD}}$, and $\mathcal{L}_{\mathcal{SPDP}'}$ denote the maximum likelihood values obtained by including the \mathcal{S} -wave and \mathcal{P} -wave components only, with the \mathcal{D} -wave added, and with both \mathcal{D} -wave and \mathcal{P}' waves added, respectively. Assuming that $\Lambda_{\mathcal{D}}$ follows a χ^2 distribution with two degrees of freedom and one degree of freedom for $\Lambda_{\mathcal{P}'}$, the \mathcal{D} and \mathcal{P}' -wave components have significances of 7.9σ and 2.5σ , respectively. Consequently, the amplitude analysis including only the \mathcal{S} , \mathcal{P} , and \mathcal{D} -wave components is taken as the nominal solution.

The nominal fit results are summarized in Table 1, with projections of the five-dimensional variables shown in Fig. 1. The fractions of the \mathcal{S} , \mathcal{P} and \mathcal{D} -wave components ($f_{\mathcal{S},\mathcal{P},\mathcal{D}}$)

are shown in Table 1. The amplitudes for waves of different spin are orthogonal and do not interfere in the total rate. The corresponding BFs are $\mathcal{B}(D^0 \rightarrow (K^-\pi^0)_{\mathcal{S}\text{-wave}} e^+\nu_e) = (0.462 \pm 0.015_{\text{stat.}} \pm 0.016_{\text{sys.}}) \times 10^{-3}$, $\mathcal{B}(D^0 \rightarrow (K^-\pi^0)_{\mathcal{P}\text{-wave}} e^+\nu_e) = (7.403 \pm 0.061_{\text{stat.}} \pm 0.048_{\text{sys.}}) \times 10^{-3}$ and $\mathcal{B}(D^0 \rightarrow (K^-\pi^0)_{\mathcal{D}\text{-wave}} e^+\nu_e) = (1.265 \pm 0.409_{\text{stat.}} \pm 0.032_{\text{sys.}}) \times 10^{-5}$. The correlation matrix for the fitted parameters is provided in Ref. [49].

Table 1. The parameters of the nominal solution, where the first and second uncertainties are statistical and systematic, respectively. No systematic uncertainty is reported for $m_{K^*(892)^-}$ due to the lack of a suitable energy calibration.

Variable	Value
$r_{\mathcal{S}}(\text{GeV})^{-1}$	$-7.53 \pm 0.22 \pm 0.11$
$r_{\mathcal{S}}^{(1)}$	$0.14 \pm 0.04 \pm 0.01$
$a_{\mathcal{S},\text{BG}}^{1/2} (\text{GeV}/c)^{-1}$	$1.98 \pm 0.10 \pm 0.13$
$b_{\mathcal{S},\text{BG}}^{1/2} (\text{GeV}/c)^{-1}$	$0.57 \pm 0.53 \pm 0.27$
$m_A (\text{GeV}/c^2)$	$2.72 \pm 0.18 \pm 0.11$
$m_V (\text{GeV}/c^2)$	$1.70 \pm 0.11 \pm 0.02$
r_V	$1.41 \pm 0.05 \pm 0.01$
r_2	$0.77 \pm 0.04 \pm 0.02$
$m_{K^*(892)^-} (\text{MeV}/c^2)$	892.9 ± 0.2
$\Gamma_{K^*(892)^-}^0 (\text{MeV})$	$47.9 \pm 0.5 \pm 0.4$
$r_{\text{BW}} (\text{GeV}/c)^{-1}$	$3.38 \pm 0.17 \pm 0.16$
$r_{\mathcal{D}} (\text{GeV})^{-4}$	$11.0 \pm 1.6 \pm 1.7$
$\phi_{\mathcal{D}} (\text{degree})$	$-16.9 \pm 7.7 \pm 3.0$
$f_{\mathcal{S}} (\%)$	$5.86 \pm 0.18 \pm 0.21$
$f_{\mathcal{P}} (\%)$	$93.97 \pm 0.19 \pm 0.21$
$f_{\mathcal{D}} (\%)$	$0.16 \pm 0.05 \pm 0.02$

We also obtain the product of $|V_{cs}|A_1(0) = 0.618 \pm 0.010_{\text{stat}} \pm 0.008_{\text{sys}}$ based on the nominal solution. The details can be found in Appendix B. Taking the $|V_{cs}| = 0.97345 \pm 0.00016$ from the global SM fit [27], we find $A_1(0) = 0.634 \pm 0.010_{\text{stat}} \pm 0.009_{\text{sys}}$.

The nominal parametrization of the \mathcal{S} -wave includes only the $K_0^*(1430)^-$ resonance explicitly. However, the lighter scalar resonance $K_0^*(700)$ is also expected to contribute to the $K\pi$ system [42–44]. Since the $K_0^*(700)$ remains a long-standing puzzle, a model-independent determination of the \mathcal{S} -wave amplitude is particularly valuable. To get the phase shift and magnitude of the \mathcal{S} -wave in a model-independent way and validate its nominal parameterization model, we perform another fit by dividing the $m_{K-\pi^0}$ spectrum into 12 bins with free phases and magnitudes of the \mathcal{S} -wave. The results are illustrated in Fig. 2; they are consistent with the nominal solution. Details are given in Ref. [49].

The systematic uncertainties in the amplitude analysis are estimated by comparing the nominal solution to those obtained by varying relevant input parameters or conditions within their uncertainties. First, the fixed parameters r_{2V} , r_{22} , as well as the mass and width of the $K_2^*(1430)^-$ are varied by ± 0.5 and $\pm 1\sigma$ [27], respectively. The background fraction f_b and the background shapes including $e^+e^- \rightarrow q\bar{q}$ and

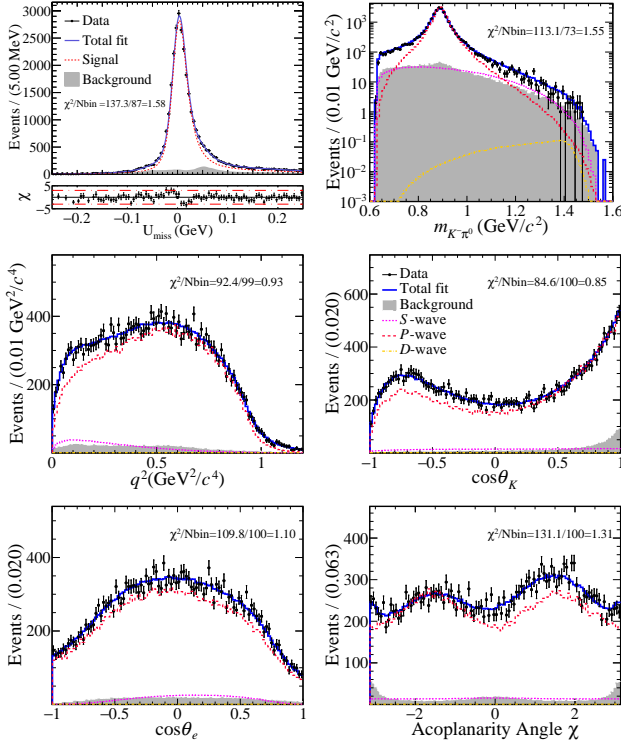


Fig. 1. The data and fits for U_{miss} and the projections onto the five kinematic variables of $D^0 \rightarrow K^-\pi^0 e^+\nu_e$ decay; The dots with error bars represent the data, the blue curves indicate the total fit, and the filled gray histograms show the background contributions. The dashed violet, dashed red, and dash-dotted orange lines correspond to the S , P , and D -wave components, respectively. Here Nbin denotes the number of bins. For the χ^2/Nbin calculation, we merge neighboring bins with very few entries until at least 20 entries are accumulated.

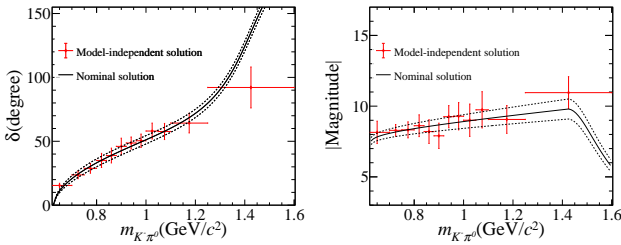


Fig. 2. S -wave phase (left) and magnitude (right) versus $m_{K^-\pi^0}$, assuming that the signal is composed of the S , P ($K^*(892)^-$) and D -wave ($K_2^*(1430)^-$). The dots with error bars represent the fit results from the model-independent measurement, and the black solid line corresponds to the nominal solution based on Table 1, while the dashed lines reflect the propagated $\pm 1\sigma$ uncertainties.

$e^+e^- \rightarrow D\bar{D}$ are also varied by $\pm 1\sigma$ based on the U_{miss} fit and Refs. [53–55], respectively. Corrections related to PID and tracking efficiencies are applied to the signal MC sample, and the resulting changes in the fits are taken as the systematic uncertainties. The relative values can be found in Ref. [49].

In summary, this Letter presents the first amplitude analysis of $D^0 \rightarrow K^-\pi^0 e^+\nu_e$ by analyzing e^+e^- annihilation

data corresponding to an integrated luminosity of 20.3 fb^{-1} collected at $\sqrt{s} = 3.773 \text{ GeV}$ with the BESIII detector. The $K_2^*(1430)^-$ component is observed for the first time with a significance of 7.9σ . The BF is measured to be $\mathcal{B}(D^0 \rightarrow K_2^*(1430)^- e^+\nu_e) = (7.603 \pm 2.457_{\text{stat}} \pm 0.194_{\text{syst}}) \times 10^{-5}$, where $\mathcal{B}(K_2^*(1430)^- \rightarrow (K\pi)^-) = (49.9 \pm 1.2)\%$ is taken from Ref. [27], assuming isospin symmetry. This result is consistent within 3σ with the predictions based on SU(3) flavor symmetry [30] and the RQM [31]. In addition, the FFs r_V and r_2 of the $D^0 \rightarrow K^*(892)^-$ transition are measured with high precision. A comparison with the PDG average [27], recent BESIII measurements [23, 25] and various theoretical calculations is shown in Fig. 3. These results help to discriminate between models, but the lack of imprecise meaning of theoretical uncertainties make precise conclusions difficult. The product of $|V_{cs}|A_1(0)$ is measured to be $0.619 \pm 0.010_{\text{stat}} \pm 0.008_{\text{syst}}$, which can provide an independent determination of the $|V_{cs}|$ to improve its precision with the theoretical input $A_1(0)$ [2]. Combining the BF of $\mathcal{B}(D^0 \rightarrow K^*(892)^-\mu^+\nu_\mu, K^*(892)^- \rightarrow K^-\pi^0) = (6.87 \pm 0.13_{\text{stat}} \pm 0.11_{\text{syst}}) \times 10^{-3}$ from the previous BESIII measurement [24], we obtain the ratio $\mathcal{R}_{\text{LFU}} = \mathcal{B}(D^0 \rightarrow K^*(892)^-\mu^+\nu_\mu)/\mathcal{B}(D^0 \rightarrow K^*(892)^-e^+\nu_e) = 0.928 \pm 0.020_{\text{stat}} \pm 0.012_{\text{syst}}$, where correlated systematic uncertainties have been canceled. This result is compatible at 2.7% precision level with the theoretical predictions in the SM 0.921-0.945 [7, 11, 12, 16]. Furthermore, by combining with $\mathcal{B}(D^0 \rightarrow K^*(892)^-e^+\nu_e, K^*(892)^- \rightarrow K_S^0\pi^-) = (6.80 \pm 0.10_{\text{stat}} \pm 0.11_{\text{syst}}) \times 10^{-3}$ from the previous BESIII measurement [23], we obtain $\mathcal{R}_{K^*-} = \mathcal{B}(K^*(892)^- \rightarrow K^-\pi^0)/\mathcal{B}(K^*(892)^- \rightarrow K_S^0\pi^-) = 1.09 \pm 0.02_{\text{stat}} \pm 0.02_{\text{syst}}$. This ratio is consistent with the value $\mathcal{R}_{K^*-} = 1.07 \pm 0.02_{\text{stat}} \pm 0.03_{\text{syst}}$, derived from the measurements in the muon channel [24, 25]. These ratio values indicate that the isospin-breaking effect in the $K^*(892)^-$ decay may need to be reconsidered, assuming the maximal breaking effect with a few percent. We also extract the phase shift of the S -wave with the $m_{K^-\pi^0}$ in a model-independent way, which provides unique insight into the nature of $K_0^*(700)$.

Acknowledgement

The BESIII Collaboration thanks the staff of BEPCII (<https://cstr.cn/31109.02.BEPC>) and the IHEP computing center for their strong support. This work is supported in part by National Key R&D Program of China under Contracts Nos. 2023YFA1606000, 2023YFA1606704; National Natural Science Foundation of China (NSFC) under Contracts Nos. 12475092, 12165022, 11635010, 11935015, 11935016, 11935018, 12025502, 12035009, 12035013, 12061131003, 12192260, 12192261, 12192262, 12192263, 12192264, 12192265, 12221005, 12225509, 12235017, 12361141819; Yunnan Fundamental Research Project under Contract No. 202301AT070162; the Chinese Academy of Sciences (CAS) Large-Scale Scientific Facility Program; the Strategic Priority Research Program of Chinese Academy of Sciences under Contract No. XDA0480600; CAS under Contract No. YSBR-101; 100 Talents Program of CAS; The Institute of

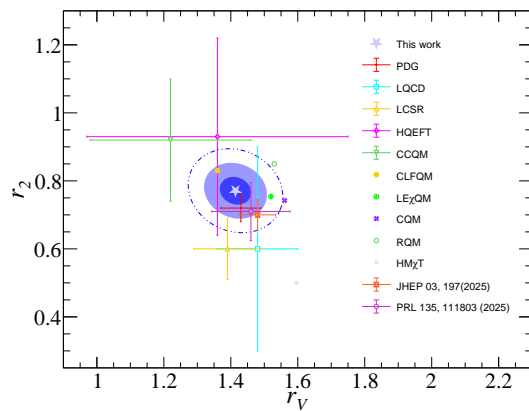


Fig. 3. Comparison of the measured FFs, PDG values and theoretical predictions from Refs. [3–15]. The inner, middle, and outer ellipses correspond to uncertainty ranges of 1σ , 2σ and 3σ deviations, respectively.

Nuclear and Particle Physics (INPAC) and Shanghai Key Laboratory for Particle Physics and Cosmology; ERC under Contract No. 758462; German Research Foundation DFG under Contract No. FOR5327; Istituto Nazionale di Fisica Nucleare, Italy; Knut and Alice Wallenberg Foundation under Contracts Nos. 2021.0174, 2021.0299; Ministry of Development of Turkey under Contract No. DPT2006K-120470; National Research Foundation of Korea under Contract No. NRF-2022R1A2C1092335; National Science and Technology fund of Mongolia; Polish National Science Centre under Contract No. 2024/53/B/ST2/00975; STFC (United Kingdom); Swedish Research Council under Contract No. 2019.04595; U. S. Department of Energy under Contract No. DE-FG02-05ER41374

[1] M. Antonelli *et al.*, *Phys. Rep.* **494**, 197 (2010).
[2] J. L. G. Santiago and G. L. Castro, [arXiv:2506.06586 \[hep-ph\]](https://arxiv.org/abs/2506.06586).
[3] D. Melikhov and B. Stech, *Phys. Rev. D* **62**, 014006 (2000).
[4] W. Y. Wang, Y. L. Wu, and M. Zhong, *Phys. Rev. D* **67**, 014024 (2003).
[5] A. Abada, D. Becirevic, P. Boucaud, J. M. Flynn, J. P. Leroy, V. Lubicz, and F. Mescia (SPQCdR Collaboration), *Nucl. Phys. B Proc. Suppl.* **119**, 625 (2003).
[6] S. Fajfer and J. Kamenik, *Phys. Rev. D* **72**, 034029 (2005).
[7] Y. L. Wu, M. Zhong, and Y. B. Zou, *Int.J.Mod.Phys.A* **21**, 6125 (2006).
[8] R. C. Verma, *J. Phys. G* **39**, 025005 (2012).
[9] T. Palmer and J. O. Eeg, *Phys. Rev. D* **89**, 034013 (2014).
[10] H. Cheng and X. Kang, *Eur. Phys. J. C* **77**, 587 (2017).
[11] N. R. Soni and J. N. Pandya, *Phys. Rev. D* **96**, 016017 (2017).
[12] M. A. Ivanov, J. G. Körner, J. N. Pandya, P. Santorelli, N. R. Soni, and C. T. Tran, *Front. Phys. (Beijing)* **14**, 64401 (2019).
[13] H. B. Fu, W. Cheng, L. Zeng, D. D. Hu, and T. Zhong, *Phys. Rev. Res.* **2**, 043129 (2020).
[14] R. N. Faustov, V. O. Galkin, and X.-W. Kang, *Phys. Rev. D* **101**, 013004 (2020).

[15] H. A. Ahmed, Y. Chen, and M. Huang, *Phys. Rev. D* **109**, 026008 (2024).
[16] W. Lin, X. E. Huang, S. Cheng, and D. L. Yao, *Phys. Rev. D* **111**, 113005 (2025).
[17] Z. Bai *et al.* (MARK-III Collaboration), *Phys. Rev. Lett.* **66**, 1011 (1991).
[18] J. M. Link *et al.* (FOCUS Collaboration), *Phys. Lett. B* **544**, 89 (2002).
[19] J. M. Link *et al.* (FOCUS Collaboration), *Phys. Lett. B* **607**, 67 (2005).
[20] P. del Amo Sanchez *et al.* (BABAR Collaboration), *Phys. Rev. D* **83**, 072001 (2011).
[21] M. Ablikim *et al.* (BESIII Collaboration), *Phys. Rev. D* **94**, 032001 (2016).
[22] M. Ablikim *et al.* (BESIII Collaboration), *JHEP* **10**, 199 (2024).
[23] M. Ablikim *et al.* (BESIII Collaboration), *JHEP* **2025**, 197 (2025).
[24] M. Ablikim *et al.* (BESIII Collaboration), *Phys. Rev. Lett.* **134**, 011803 (2025).
[25] M. Ablikim *et al.* (BESIII Collaboration), *Phys. Rev. Lett.* **135**, 111803 (2025).
[26] M. Ablikim *et al.* (BESIII Collaboration), *Phys. Rev. Lett.* **135**, 171801 (2025).
[27] S. Navas *et al.* (Particle Data Group), *Phys. Rev. D* **110**, 030001 (2024), and 2025 update.
[28] M. Ablikim (BESIII Collaboration), *Chin. Phys. C* **37**, 123001 (2013).
[29] M. Ablikim *et al.* (BESIII Collaboration), *Chin. Phys. C* **48**, 123001 (2024).
[30] Y. Qiao, Y. X. Liu, Y. G. Xu, and R. M. Wang, *Eur. Phys. J. C* **84**, 1110 (2024).
[31] V. O. Galkin and I. S. Sukhanov, *Phys. Rev. D* **111**, 093001 (2025).
[32] J. P. Lees *et al.* (BABAR Collaboration), *Phys. Rev. Lett.* **109**, 101802 (2012).
[33] J. P. Lees *et al.* (BABAR Collaboration), *Phys. Rev. D* **88**, 072012 (2013).
[34] R. Aaij *et al.* (LHCb Collaboration), *Phys. Rev. Lett.* **113**, 151601 (2014).
[35] M. Huschle *et al.* (Belle Collaboration), *Phys. Rev. D* **92**, 072014 (2015).
[36] R. Aaij *et al.* (LHCb Collaboration), *JHEP* **08**, 55 (2017).
[37] M. Alston, L. W. Alvarez, P. Eberhard, M. L. Good, W. Graziano, H. K. Ticho, and S. G. Wojcicki, *Phys. Rev. Lett.* **6**, 300 (1961).
[38] D. L. Yao, L. Y. Dai, H. Q. Zheng, and Z. Y. Zhou, *Rept. Prog. Phys.* **84**, 076201 (2021).
[39] R. L. Jaffe, *Phys. Rept.* **409**, 1 (2005).
[40] M. R. Pennington, *AIP Conf. Proc.* **1257**, 27 (2010).
[41] J. R. Pelaez and A. Rodas, *Phys. Rev. D* **93**, 074025 (2016).
[42] Z. Y. Zhou and H. Q. Zheng, *Nucl. Phys. A* **775**, 212 (2006).
[43] S. Descotes-Genon and B. Moussallam, *Eur. Phys. J. C* **48**, 553 (2006).
[44] C. B. Lang, L. Leskovec, D. Mohler, and S. Prelovsek, *Phys. Rev. D* **86**, 054508 (2012).
[45] D. Aston *et al.*, *Nucl. Phys. B* **296**, 493 (1988).
[46] P. Estabrooks, R. Carnegie, A. Martin, W. Dunwoodie, T. Lasinski, and D. Leith, *Nucl. Phys. B* **133**, 490 (1978).
[47] M. Ablikim *et al.* (BESIII Collaboration), *Nucl. Instrum. Meth. A* **614**, 345 (2010).
[48] K. X. Huang, Z. J. Li, Z. Qian, J. Zhu, H. Y. Li, Y. M. Zhang, S. S. Sun, and Z. Y. You, *NUCL SCI TECH* **33**, 142 (2022).
[49] See Supplemental Material for additional analysis information.
[50] C. L. Y. Lee, M. Lu, and M. B. Wise, *Phys. Rev. D* **46**, 5040

(1992).

- [51] A. K. Leibovich, Z. Ligeti, I. W. Stewart, and M. B. Wise, *Phys. Rev. D* **57**, 308 (1998).
- [52] J. Charles, A. Le Yaouanc, L. Oliver, O. Pene, and J. C. Raynal, *Phys. Rev. D* **60**, 014001 (1999).
- [53] M. Ablikim *et al.* (BESIII Collaboration), *Chin. Phys. C* **42**, 083001 (2018).
- [54] M. Ablikim *et al.* (BES Collaboration), *Phys. Rev. D* **76**, 122002 (2007).
- [55] M. Ablikim *et al.* (BES Collaboration), *Phys. Lett. B* **641**, 145 (2006).

Appendix A: Branching fraction in DT method

Based on the DT method, the BF of the $D^0 \rightarrow K^-\pi^0 e^+\nu_e$ decay is expressed as

$$\mathcal{B}_{\text{SL}} = \frac{N_{\text{DT}}}{N_{\text{ST}}^{\text{tot}} \bar{\epsilon}_{\text{SL}}}, \quad (2)$$

where N_{DT} and $N_{\text{ST}}^{\text{tot}} = \sum_{i=1}^3 N_{\text{ST}}^i$ are the total DT and ST yields summing over all tag modes, respectively. $\bar{\epsilon}_{\text{SL}} = \sum_{i=1}^3 \frac{N_{\text{ST}}^i}{N_{\text{ST}}^{\text{tot}}} \frac{\epsilon_{\text{DT}}^i}{\epsilon_{\text{ST}}^i}$ is the averaged efficiency of reconstructing the $D^0 \rightarrow K^-\pi^0 e^+\nu_e$ decay, where ϵ_{DT}^i and ϵ_{ST}^i are the DT and ST efficiencies for the i^{th} tag mode, respectively.

Appendix B: Extracting the product of $|V_{cs}|A_1(0)$

The differential decay width of the \mathcal{P} -wave $K^*(892)^-$ is integrated over three angles yielding

$$\frac{d\Gamma}{dq^2 dm_{K^-\pi^0}^2} = \frac{1}{3} \frac{G_F^2 |V_{cs}|^2}{(4\pi)^5 m_{D^0}^2} \beta p_{K^-\pi^0} \left[\frac{2}{3} \left\{ |\mathcal{F}_{11}|^2 + |\mathcal{F}_{21}|^2 + |\mathcal{F}_{31}|^2 \right\} \right]. \quad (3)$$

In this expression, G_F is the Fermi coupling constant, m_D is the mass of D^0 meson, V_{cs} is the $c \rightarrow s$ CKM matrix element, \mathcal{F}_{i1} are the FF terms corresponding to the \mathcal{P} wave component, and $\beta = 2p^*/m_{K^-\pi^0}$, where p^* is the momentum of K^- in the $K^-\pi^0$ rest frame and $p_{K^-\pi^0}$ is the momentum of the $K^-\pi^0$ system in the D^0 rest frame.

Replacing The \mathcal{F}_{i1} in Eq.(3) with helicity FFs transforms this decay width into

$$\frac{d\Gamma}{dq^2 dm_{K^-\pi^0}^2} = \frac{G_F^2 |V_{cs}|^2}{96\pi^4 m_{D^0}^2} \frac{p^* \mathcal{B}_{K^*}}{m_{K^-\pi^0}} \frac{p_{K\pi} q^2}{p_0^* \Gamma_0} \left(|H_0|^2 + |H_+|^2 + |H_-|^2 \right) |\mathcal{A}(m_{K^-\pi^0})|^2. \quad (4)$$

Here, $\mathcal{B}_{K^*} = 0.354 \pm 0.006$ denotes the BF of $K^*(892)^- \rightarrow K^-\pi^0$ considering the ratio \mathcal{R}_{K^*} measured in this Letter. The amplitude-squared term $|\mathcal{A}(m_{K^-\pi^0})|^2$ describing the $K^*(892)^-$ is given by

$$|\mathcal{A}(m_{K^-\pi^0})|^2 = \frac{(m_0 \Gamma_0 F_1(m_{K^-\pi^0}))^2}{(m_0^2 - m_{K^-\pi^0}^2)^2 + (m_0 \Gamma(m_{K^-\pi^0}))^2}, \quad (5)$$

where m_0 and Γ_0 are the mass and width of $K^*(892)^-$, respectively, $F_1(m_{K^-\pi^0}) = \left(\frac{p^*}{p_0^*}\right) \frac{B_1(p^*)}{B_1(p_0^*)}$ with the Blatt-Weisskopf damping factor $B_1(p^*) = 1/\sqrt{1 - r_{\text{BW}} p^*}$. The decay width is

$$\Gamma = \frac{\hbar \mathcal{B}(D^0 \rightarrow K^*(892)^- e^+\nu_e) \mathcal{B}(K^*(892)^- \rightarrow K^-\pi^0)}{\tau_{D^0}}, \quad (6)$$

where τ_{D^0} is the lifetime of D^0 meson, \hbar is the Planck constant, and the BF product is measured in this analysis.

Finally, by constraining to the decay width, a two-dimensional integration of Eq. (4) is performed with the parameters from the nominal solution to extract the product of $|V_{cs}|A_1(0)$. The systematical are mainly produced from the amplitude analysis solution and the uncertainty from PDG value.

- M. Ablikim¹, M. N. Achasov^{4,b}, P. Adlarson⁸¹, X. C. Ai⁸⁶, R. Aliberti³⁸, A. Amoroso^{80A,80C}, Q. An^{77,63,†}, Y. Bai⁶¹, O. Bakina³⁹, Y. Ban^{49,g}, H.-R. Bao⁶⁹, V. Batozskaya^{1,47}, K. Begzsuren³⁵, N. Berger³⁸, M. Berlowski⁴⁷, M. B. Bertani^{30A}, D. Bettoni^{31A}, F. Bianchi^{80A,80C}, E. Bianco^{80A,80C}, A. Bortone^{80A,80C}, I. Boyko³⁹, R. A. Briere⁵, A. Brueggemann⁷⁴, H. Cai⁸², M. H. Cai^{41,j,k}, X. Cai^{1,63}, A. Calcaterra^{30A}, G. F. Cao^{1,69}, N. Cao^{1,69}, S. A. Cetin^{67A}, X. Y. Chai^{49,g}, J. F. Chang^{1,63}, T. T. Chang⁴⁶, G. R. Che⁴⁶, Y. Z. Che^{1,63,69}, C. H. Chen¹⁰, Chao Chen⁵⁹, G. Chen¹, H. S. Chen^{1,69}, H. Y. Chen²¹, M. L. Chen^{1,63,69}, S. J. Chen⁴⁵, S. M. Chen⁶⁶, T. Chen^{1,69}, X. R. Chen^{34,69}, X. T. Chen^{1,69}, X. Y. Chen^{12,f}, Y. B. Chen¹⁶, Y. Q. Chen⁶⁴, Haoyang Cheng²⁷, J. C. Cheng⁴⁸, L. N. Cheng⁴⁶, S. K. Choi¹¹, X. S. Chu^{12,f}, G. Cibinetto^{31A}, F. Cossio^{80C}, J. Cottee-Meldrum⁶⁸, H. L. Dai^{1,63}, J. P. Dai⁸⁴, Lingyun Dai^{27,h}, X. C. Dai⁶⁶, A. Dbeysy¹⁹, R. E. de Boer³, D. Dedovich³⁹, C. Q. Deng⁷⁸, Z. Y. Deng¹, A. Denig³⁸, I. Denisenko³⁹, M. Destefanis^{80A,80C}, F. De Mori^{80A,80C}, X. X. Ding^{49,g}, Y. Ding⁴³, Y. X. Ding³², J. Dong^{1,63}, L. Y. Dong^{1,69}, M. Y. Dong^{1,63,69}, X. Dong⁸², M. C. Du¹, S. X. Du⁸⁶, S. X. Du^{12,f}, X. L. Du⁸⁶, Y. Y. Duan⁵⁹, Z. H. Duan⁴⁵, P. Egorov^{39,a}, G. F. Fan⁴⁵, J. J. Fan²⁰, Y. H. Fan⁴⁸, J. Fang^{1,63}, J. Fang⁶⁴, S. S. Fang^{1,69}, W. X. Fang¹, Y. Q. Fang^{1,63,†}, L. Fava^{80B,80C}, F. Feldbauer³, G. Felici^{30A}, C. Q. Feng^{77,63}, J. H. Feng¹⁶, L. Feng^{41,j,k}, Q. X. Feng^{41,j,k}, Y. T. Feng^{77,63}, M. Fritsch³, C. D. Fu¹, J. L. Fu⁶⁹, Y. W. Fu^{1,69}, H. Gao⁶⁹, Y. Gao^{77,63}, Y. N. Gao^{49,g}, Y. N. Gao²⁰, Y. Y. Gao³², Z. Gao⁴⁶, S. Garbolino^{80C}, I. Garzia^{31A,31B}, L. Ge⁶¹, P. T. Ge²⁰, Z. W. Ge⁴⁵, C. Geng⁶⁴, E. M. Gersabeck⁷³, A. Gilman⁷⁵, K. Goetzen¹³, J. D. Gong³⁷,

L. Gong⁴³ , W. X. Gong^{1,63} , W. Gradl³⁸ , S. Gramigna^{31A,31B} , M. Greco^{80A,80C} , M. D. Gu⁵⁴ , M. H. Gu^{1,63} ,
C. Y. Guan^{1,69} , A. Q. Guo³⁴ , J. N. Guo^{12,f} , L. B. Guo⁴⁴ , M. J. Guo⁵³ , R. P. Guo⁵² , X. Guo⁵³ , Y. P. Guo^{12,f} ,
A. Guskov^{39,a} , J. Gutierrez²⁹ , T. T. Han¹ , F. Hanisch³ , K. D. Hao^{77,63} , X. Q. Hao²⁰ , F. A. Harris⁷¹ , C. Z. He^{49,g} ,
K. L. He^{1,69} , F. H. Heinsius³ , C. H. Heinz³⁸ , Y. K. Heng^{1,63,69} , C. Herold⁶⁵ , P. C. Hong³⁷ , G. Y. Hou^{1,69} ,
X. T. Hou^{1,69} , Y. R. Hou⁶⁹ , Z. L. Hou¹ , H. M. Hu^{1,69} , J. F. Hu^{60,i} , Q. P. Hu^{77,63} , S. L. Hu^{12,f} , T. Hu^{1,63,69} , Y. Hu¹ ,
Z. M. Hu⁶⁴ , G. S. Huang^{77,63} , K. X. Huang⁶⁴ , L. Q. Huang^{34,69} , P. Huang⁴⁵ , X. T. Huang⁵³ , Y. P. Huang¹ ,
Y. S. Huang⁶⁴ , T. Hussain⁷⁹ , N. Hüsken³⁸ , N. in der Wiesche⁷⁴ , J. Jackson²⁹ , Q. Ji¹ , Q. P. Ji²⁰ , W. Ji^{1,69} ,
X. B. Ji^{1,69} , X. L. Ji^{1,63} , X. Q. Jia⁵³ , Z. K. Jia^{77,63} , D. Jiang^{1,69} , H. B. Jiang⁸² , P. C. Jiang^{49,g} , S. J. Jiang¹⁰ ,
X. S. Jiang^{1,63,69} , Y. J. Jiang⁶⁹ , J. B. Jiao⁵³ , J. K. Jiao³⁷ , Z. Jiao²⁵ , S. Jin⁴⁵ , Y. Jin⁷² , M. Q. Jing^{1,69} , X. M. Jing⁶⁹ ,
T. Johansson⁸¹ , S. Kabana³⁶ , N. Kalantar-Nayestanaki⁷⁰ , X. L. Kang¹⁰ , X. S. Kang⁴³ , M. Kavatsyuk⁷⁰ , B. C. Ke⁸⁶ ,
V. Khachatryan²⁹ , A. Khoukaz⁷⁴ , O. B. Kolcu^{67A} , B. Kopf³ , L. Kröger⁷⁴ , M. Kuessner³ , X. Kui^{1,69} , N. Kumar²⁸ ,
A. Kupsc^{47,81} , W. Kühn⁴⁰ , Q. Lan⁷⁸ , W. N. Lan²⁰ , T. T. Lei^{77,63} , M. Lellmann³⁸ , T. Lenz³⁸ , C. Li⁵⁰ , C. Li⁴⁶ ,
C. H. Li⁴⁴ , C. K. Li²¹ , D. M. Li⁸⁶ , F. Li^{1,63} , G. Li¹ , H. B. Li^{1,69} , H. J. Li²⁰ , H. L. Li⁸⁶ , H. N. Li^{60,i} , Hui Li⁴⁶ ,
J. R. Li⁶⁶ , J. S. Li⁶⁴ , J. W. Li⁵³ , K. Li¹ , K. L. Li^{41,j,k} , L. J. Li^{1,69} , Lei Li⁵¹ , M. H. Li⁴⁶ , M. R. Li^{1,69} , P. L. Li⁶⁹ ,
P. R. Li^{41,j,k} , Q. M. Li^{1,69} , Q. X. Li⁵³ , R. Li^{18,34} , S. X. Li¹² , Shanshan Li^{27,h} , T. Li⁵³ , T. Y. Li⁴⁶ , W. D. Li^{1,69} ,
W. G. Li^{1,†} , X. L. Li^{1,69} , X. H. Li^{77,63} , X. K. Li^{49,g} , X. L. Li⁵³ , X. Y. Li^{1,9} , X. Z. Li⁶⁴ , Y. Li²⁰ , Y. G. Li^{49,g} ,
Y. P. Li³⁷ , Z. H. Li⁴¹ , Z. J. Li⁶⁴ , Z. X. Li⁴⁶ , Z. Y. Li⁸⁴ , C. Liang⁴⁵ , H. Liang^{77,63} , Y. F. Liang⁵⁸ , Y. T. Liang^{34,69} ,
G. R. Liao¹⁴ , L. B. Liao⁶⁴ , M. H. Liao⁶⁴ , Y. P. Liao^{1,69} , J. Libby²⁸ , A. Limphirat⁶⁵ , D. X. Lin^{34,69} , L. Q. Lin⁴² ,
T. Lin¹ , B. J. Liu¹ , B. X. Liu⁸² , C. X. Liu¹ , F. Liu¹ , F. H. Liu⁵⁷ , Feng Liu⁶ , G. M. Liu^{60,i} , H. Liu^{41,j,k} ,
H. B. Liu¹⁵ , H. H. Liu¹ , H. M. Liu^{1,69} , Huihui Liu²² , J. B. Liu^{77,63} , J. J. Liu²¹ , K. Liu^{41,j,k} , K. Liu⁷⁸ , K. Y. Liu⁴³ ,
Ke Liu²³ , L. Liu⁴¹ , L. C. Liu⁴⁶ , Lu Liu⁴⁶ , M. H. Liu³⁷ , P. L. Liu¹ , Q. Liu⁶⁹ , S. B. Liu^{77,63} , W. M. Liu^{77,63} ,
W. T. Liu⁴² , X. Liu^{41,j,k} , X. K. Liu^{41,j,k} , X. L. Liu^{12,f} , X. Y. Liu⁸² , Y. Liu^{41,j,k} , Y. Liu⁸⁶ , Y. B. Liu⁴⁶ ,
Z. A. Liu^{1,63,69} , Z. D. Liu¹⁰ , Z. Q. Liu⁵³ , Z. Y. Liu⁴¹ , X. C. Lou^{1,63,69} , H. J. Lu²⁵ , J. G. Lu^{1,63} , X. L. Lu¹⁶ , Y. Lu⁷ ,
Y. H. Lu^{1,69} , Y. P. Lu^{1,63} , Z. H. Lu^{1,69} , C. L. Luo⁴⁴ , J. R. Luo⁶⁴ , J. S. Luo^{1,69} , M. X. Luo⁸⁵ , T. Luo^{12,f} , X. L. Luo^{1,63} ,
Z. Y. Lv²³ , X. R. Lyu^{69,n} , Y. F. Lyu⁴⁶ , Y. H. Lyu⁸⁶ , F. C. Ma⁴³ , H. L. Ma¹ , J. L. Ma^{1,69} , L. L. Ma⁵³ ,
L. R. Ma⁷² , Q. M. Ma¹ , R. Q. Ma^{1,69} , R. Y. Ma²⁰ , T. Ma^{77,63} , X. T. Ma^{1,69} , X. Y. Ma^{1,63} , Y. M. Ma³⁴ ,
F. E. Maas¹⁹ , I. MacKay⁷⁵ , M. Maggiora^{80A,80C} , S. Malde⁷⁵ , Q. A. Malik⁷⁹ , H. X. Mao^{41,j,k} , Y. J. Mao^{49,g} ,
Z. P. Mao¹ , S. Marcello^{80A,80C} , A. Marshall⁶⁸ , F. M. Melendi^{31A,31B} , Y. H. Meng⁶⁹ , Z. X. Meng⁷² , G. Mezzadri^{31A} ,
H. Miao^{1,69} , T. J. Min⁴⁵ , R. E. Mitchell²⁹ , X. H. Mo^{1,63,69} , B. Moses²⁹ , N. Yu. Muchnoi^{4,b} , J. Muskalla³⁸ ,
Y. Nefedov³⁹ , F. Nerling^{19,d} , H. Neuwirth⁷⁴ , Z. Ning^{1,63} , S. Nisar³³ , Q. L. Niu^{41,j,k} , W. D. Niu^{12,f} , Y. Niu⁵³ ,
C. Normand⁶⁸ , S. L. Olsen^{11,69} , Q. Ouyang^{1,63,69} , S. Pacetti^{30B,30C} , X. Pan⁵⁹ , Y. Pan⁶¹ , A. Pathak¹¹ , Y. P. Pei^{77,63} ,
M. Pelizaeus³ , H. P. Peng^{77,63} , X. J. Peng^{41,j,k} , Y. Y. Peng^{41,j,k} , K. Peters^{13,d} , K. Petridis⁶⁸ , J. L. Ping⁴⁴ ,
R. G. Ping^{1,69} , S. Plura³⁸ , V. Prasad³⁷ , F. Z. Qi¹ , H. R. Qi⁶⁶ , M. Qi⁴⁵ , S. Qian^{1,63} , W. B. Qian⁶⁹ , C. F. Qiao⁶⁹ ,
J. H. Qiao²⁰ , J. J. Qin⁷⁸ , J. L. Qin⁵⁹ , L. Q. Qin¹⁴ , L. Y. Qin^{77,63} , P. B. Qin⁷⁸ , X. P. Qin⁴² , X. S. Qin⁵³ ,
Z. H. Qin^{1,63} , J. F. Qiu¹ , Z. H. Qu⁷⁸ , J. Rademacker⁶⁸ , C. F. Redmer³⁸ , A. Rivetti^{80C} , M. Rolo^{80C} , G. Rong^{1,69} ,
S. S. Rong^{1,69}

P. Zhang^{1,9} , Q. Zhang²⁰ , Q. Y. Zhang³⁷ , R. Y. Zhang^{41,j,k} , S. H. Zhang^{1,69} , Shulei Zhang^{27,h} , X. M. Zhang¹ ,
X. Y. Zhang⁵³ , Y. Zhang¹ , Y. Zhang⁷⁸ , Y. T. Zhang⁸⁶ , Y. H. Zhang^{1,63} , Y. P. Zhang^{77,63} , Z. D. Zhang¹ , Z. H. Zhang¹ ,
Z. L. Zhang³⁷ , Z. L. Zhang⁵⁹ , Z. X. Zhang²⁰ , Z. Y. Zhang⁸² , Z. Y. Zhang⁴⁶ , Z. Z. Zhang⁴⁸ , Zh. Zh. Zhang²⁰ ,
G. Zhao¹ , J. Y. Zhao^{1,69} , J. Z. Zhao^{1,63} , L. Zhao¹ , L. Zhao^{77,63} , M. G. Zhao⁴⁶ , S. J. Zhao⁸⁶ , Y. B. Zhao^{1,63} ,
Y. L. Zhao⁵⁹ , Y. X. Zhao^{34,69} , Z. G. Zhao^{77,63} , A. Zhemchugov^{39,a} , B. Zheng⁷⁸ , B. M. Zheng³⁷ , J. P. Zheng^{1,63} ,
W. J. Zheng^{1,69} , X. R. Zheng²⁰ , Y. H. Zheng^{69,n} , B. Zhong⁴⁴ , C. Zhong²⁰ , H. Zhou^{38,53,m} , J. Q. Zhou³⁷ , S. Zhou⁶ ,
X. Zhou⁸² , X. K. Zhou⁶ , X. R. Zhou^{77,63} , X. Y. Zhou⁴² , Y. X. Zhou⁸³ , Y. Z. Zhou^{12,f} , A. N. Zhu⁶⁹ , J. Zhu⁴⁶ ,
K. Zhu¹ , K. J. Zhu^{1,63,69} , K. S. Zhu^{12,f} , L. Zhu³⁷ , L. X. Zhu⁶⁹ , S. H. Zhu⁷⁶ , T. J. Zhu^{12,f} , W. D. Zhu^{12,f} ,
W. J. Zhu¹ , W. Z. Zhu²⁰ , Y. C. Zhu^{77,63} , Z. A. Zhu^{1,69} , X. Y. Zhuang⁴⁶ , J. H. Zou¹ , J. Zu^{77,63} 

(BESIII Collaboration)

¹ Institute of High Energy Physics, Beijing 100049, People's Republic of China

² Beihang University, Beijing 100191, People's Republic of China

³ Bochum Ruhr-University, D-44780 Bochum, Germany

⁴ Budker Institute of Nuclear Physics SB RAS (BINP), Novosibirsk 630090, Russia

⁵ Carnegie Mellon University, Pittsburgh, Pennsylvania 15213, USA

⁶ Central China Normal University, Wuhan 430079, People's Republic of China

⁷ Central South University, Changsha 410083, People's Republic of China

⁸ Chengdu University of Technology, Chengdu 610059, People's Republic of China

⁹ China Center of Advanced Science and Technology, Beijing 100190, People's Republic of China

¹⁰ China University of Geosciences, Wuhan 430074, People's Republic of China

¹¹ Chung-Ang University, Seoul, 06974, Republic of Korea

¹² Fudan University, Shanghai 200433, People's Republic of China

¹³ GSI Helmholtzcentre for Heavy Ion Research GmbH, D-64291 Darmstadt, Germany

¹⁴ Guangxi Normal University, Guilin 541004, People's Republic of China

¹⁵ Guangxi University, Nanning 530004, People's Republic of China

¹⁶ Guangxi University of Science and Technology, Liuzhou 545006, People's Republic of China

¹⁷ Hangzhou Normal University, Hangzhou 310036, People's Republic of China

¹⁸ Hebei University, Baoding 071002, People's Republic of China

¹⁹ Helmholtz Institute Mainz, Staudinger Weg 18, D-55099 Mainz, Germany

²⁰ Henan Normal University, Xinxiang 453007, People's Republic of China

²¹ Henan University, Kaifeng 475004, People's Republic of China

²² Henan University of Science and Technology, Luoyang 471003, People's Republic of China

²³ Henan University of Technology, Zhengzhou 450001, People's Republic of China

²⁴ Hengyang Normal University, Hengyang 421001, People's Republic of China

²⁵ Huangshan College, Huangshan 245000, People's Republic of China

²⁶ Hunan Normal University, Changsha 410081, People's Republic of China

²⁷ Hunan University, Changsha 410082, People's Republic of China

²⁸ Indian Institute of Technology Madras, Chennai 600036, India

²⁹ Indiana University, Bloomington, Indiana 47405, USA

³⁰ INFN Laboratori Nazionali di Frascati, (A)INFN Laboratori Nazionali di Frascati, I-00044, Frascati, Italy; (B)INFN Sezione di Perugia, I-06100, Perugia, Italy; (C)University of Perugia, I-06100, Perugia, Italy

³¹ INFN Sezione di Ferrara, (A)INFN Sezione di Ferrara, I-44122, Ferrara, Italy; (B)University of Ferrara, I-44122, Ferrara, Italy

³² Inner Mongolia University, Hohhot 010021, People's Republic of China

³³ Institute of Business Administration, University Road, Karachi, 75270 Pakistan

³⁴ Institute of Modern Physics, Lanzhou 730000, People's Republic of China

³⁵ Institute of Physics and Technology, Mongolian Academy of Sciences, Peace Avenue 54B, Ulaanbaatar 13330, Mongolia

³⁶ Instituto de Alta Investigación, Universidad de Tarapacá, Casilla 7D, Arica 1000000, Chile

³⁷ Jilin University, Changchun 130012, People's Republic of China

³⁸ Johannes Gutenberg University of Mainz, Johann-Joachim-Becher-Weg 45, D-55099 Mainz, Germany

³⁹ Joint Institute for Nuclear Research, 141980 Dubna, Moscow region, Russia

⁴⁰ Justus-Liebig-Universität Giessen, II. Physikalisches Institut, Heinrich-Buff-Ring 16, D-35392 Giessen, Germany

⁴¹ Lanzhou University, Lanzhou 730000, People's Republic of China

⁴² Liaoning Normal University, Dalian 116029, People's Republic of China

⁴³ Liaoning University, Shenyang 110036, People's Republic of China

⁴⁴ Nanjing Normal University, Nanjing 210023, People's Republic of China

⁴⁵ Nanjing University, Nanjing 210093, People's Republic of China

⁴⁶ Nankai University, Tianjin 300071, People's Republic of China

⁴⁷ National Centre for Nuclear Research, Warsaw 02-093, Poland

⁴⁸ North China Electric Power University, Beijing 102206, People's Republic of China

⁴⁹ Peking University, Beijing 100871, People's Republic of China

⁵⁰ Qufu Normal University, Qufu 273165, People's Republic of China

⁵¹ Renmin University of China, Beijing 100872, People's Republic of China

- ⁵² Shandong Normal University, Jinan 250014, People's Republic of China
- ⁵³ Shandong University, Jinan 250100, People's Republic of China
- ⁵⁴ Shandong University of Technology, Zibo 255000, People's Republic of China
- ⁵⁵ Shanghai Jiao Tong University, Shanghai 200240, People's Republic of China
- ⁵⁶ Shanxi Normal University, Linfen 041004, People's Republic of China
- ⁵⁷ Shanxi University, Taiyuan 030006, People's Republic of China
- ⁵⁸ Sichuan University, Chengdu 610064, People's Republic of China
- ⁵⁹ Soochow University, Suzhou 215006, People's Republic of China
- ⁶⁰ South China Normal University, Guangzhou 510006, People's Republic of China
- ⁶¹ Southeast University, Nanjing 211100, People's Republic of China
- ⁶² Southwest University of Science and Technology, Mianyang 621010, People's Republic of China
- ⁶³ State Key Laboratory of Particle Detection and Electronics, Beijing 100049, Hefei 230026, People's Republic of China
- ⁶⁴ Sun Yat-Sen University, Guangzhou 510275, People's Republic of China
- ⁶⁵ Suranaree University of Technology, University Avenue 111, Nakhon Ratchasima 30000, Thailand
- ⁶⁶ Tsinghua University, Beijing 100084, People's Republic of China
- ⁶⁷ Turkish Accelerator Center Particle Factory Group, (A)Istinye University, 34010, Istanbul, Turkey; (B)Near East University, Nicosia, North Cyprus, 99138, Mersin 10, Turkey
- ⁶⁸ University of Bristol, H H Wills Physics Laboratory, Tyndall Avenue, Bristol, BS8 1TL, UK
- ⁶⁹ University of Chinese Academy of Sciences, Beijing 100049, People's Republic of China
- ⁷⁰ University of Groningen, NL-9747 AA Groningen, The Netherlands
- ⁷¹ University of Hawaii, Honolulu, Hawaii 96822, USA
- ⁷² University of Jinan, Jinan 250022, People's Republic of China
- ⁷³ University of Manchester, Oxford Road, Manchester, M13 9PL, United Kingdom
- ⁷⁴ University of Muenster, Wilhelm-Klemm-Strasse 9, 48149 Muenster, Germany
- ⁷⁵ University of Oxford, Keble Road, Oxford OX13RH, United Kingdom
- ⁷⁶ University of Science and Technology Liaoning, Anshan 114051, People's Republic of China
- ⁷⁷ University of Science and Technology of China, Hefei 230026, People's Republic of China
- ⁷⁸ University of South China, Hengyang 421001, People's Republic of China
- ⁷⁹ University of the Punjab, Lahore-54590, Pakistan
- ⁸⁰ University of Turin and INFN, (A)University of Turin, I-10125, Turin, Italy; (B)University of Eastern Piedmont, I-15121, Alessandria, Italy; (C)INFN, I-10125, Turin, Italy
- ⁸¹ Uppsala University, Box 516, SE-75120 Uppsala, Sweden
- ⁸² Wuhan University, Wuhan 430072, People's Republic of China
- ⁸³ Yantai University, Yantai 264005, People's Republic of China
- ⁸⁴ Yunnan University, Kunming 650500, People's Republic of China
- ⁸⁵ Zhejiang University, Hangzhou 310027, People's Republic of China
- ⁸⁶ Zhengzhou University, Zhengzhou 450001, People's Republic of China
- † Deceased
- ^a Also at the Moscow Institute of Physics and Technology, Moscow 141700, Russia
- ^b Also at the Novosibirsk State University, Novosibirsk, 630090, Russia
- ^c Also at the NRC "Kurchatov Institute", PNPI, 188300, Gatchina, Russia
- ^d Also at Goethe University Frankfurt, 60323 Frankfurt am Main, Germany
- ^e Also at Key Laboratory for Particle Physics, Astrophysics and Cosmology, Ministry of Education; Shanghai Key Laboratory for Particle Physics and Cosmology; Institute of Nuclear and Particle Physics, Shanghai 200240, People's Republic of China
- ^f Also at Key Laboratory of Nuclear Physics and Ion-beam Application (MOE) and Institute of Modern Physics, Fudan University, Shanghai 200443, People's Republic of China
- ^g Also at State Key Laboratory of Nuclear Physics and Technology, Peking University, Beijing 100871, People's Republic of China
- ^h Also at School of Physics and Electronics, Hunan University, Changsha 410082, China
- ⁱ Also at Guangdong Provincial Key Laboratory of Nuclear Science, Institute of Quantum Matter, South China Normal University, Guangzhou 510006, China
- ^j Also at MOE Frontiers Science Center for Rare Isotopes, Lanzhou University, Lanzhou 730000, People's Republic of China
- ^k Also at Lanzhou Center for Theoretical Physics, Lanzhou University, Lanzhou 730000, People's Republic of China
- ^l Also at Ecole Polytechnique Federale de Lausanne (EPFL), CH-1015 Lausanne, Switzerland
- ^m Also at Helmholtz Institute Mainz, Staudinger Weg 18, D-55099 Mainz, Germany
- ⁿ Also at Hangzhou Institute for Advanced Study, University of Chinese Academy of Sciences, Hangzhou 310024, China
- ^o Currently at Silesian University in Katowice, Chorzow, 41-500, Poland
- ^p Also at Applied Nuclear Technology in Geosciences Key Laboratory of Sichuan Province, Chengdu University of Technology, Chengdu 610059, People's Republic of China